Molecular Pharmacology Fast Forward. Published on February 18, 2016 as DOI: 10.1124/mol.115.102079
This article has not been copyedited and formatted. The final version may differ from this version.

Generation and Characterization of a Breast Cancer Resistance Protein Humanized Mouse Model

Shannon Dallas, Laurent Salphati, David Gomez-Zepeda, Thomas Wanek, Liangfu Chen, Xiaoyan Chu, Jeevan Kunta, Mario Mezler, Marie-Claude Menet, Stephanie Chasseigneaux, Xavier Declèves, Oliver Langer, Esaie Pierre, Karen DiLoreto, Carolin Hoft, Loic Laplanche, Jodie Pang, Tony Pereira, Clara Andonian, Damir Simic, Anja Rode, Jocelyn Yabut, Xiaolin Zhang and Nico Scheer

DMPK and Bioanalytical Research, Abbvie Deutschland GmbH & Co. KG, Ludwigshafen, Germany (MM, CH, LL).

Drug Metabolism and Pharmacokinetics, Genentech, Inc., 1 DNA Way, South San Francisco, CA 94080, USA (LS, JP, XZ)

Drug Metabolism and Pharmacokinetics, GlaxoSmithKline Pharmaceuticals, King of Prussia, Pennsylvania, USA (LC, CA, EP)

Health and Environment Department, AIT Austrian Institute of Technology GmbH, A-2444 Seibersdorf, Austria (TW, OL); Department of Clinical Pharmacology, Medical University of Vienna, Vienna, Austria (OL)

Preclinical Development & Safety, Janssen Research & Development, LLC, Spring House, PA, USA (SD, JK[1], KD, DS).

Merck Sharp & Dohme Corporation, Whitehouse Station, New Jersey, USA (XC, TP, JY)

Université Paris Descartes, UMR-S 1144, Paris, France (DGZ, MCM, SC, XD)

Taconic Biosciences GmbH, Neurather Ring 1, Koeln 51063, Germany (AR, NS); Current affiliation of AR and NS: Independent consultants, Cologne, Germany.

[1]Current affiliation: Discovery and Product Development, Teva Pharmaceuticals Research & Development, West Chester, PA, USA

Molecular Pharmacology Fast Forward. Published on February 18, 2016 as DOI: 10.1124/mol.115.102079
This article has not been copyedited and formatted. The final version may differ from this version.

Running title: BCRP humanized mice

Address correspondence to:

Laurent Salphati, Pharm.D., PhD, Department of Drug Metabolism and Pharmacokinetics, Genentech, Inc., 1 DNA Way, South San Francisco, CA 94080, USA.

Tel.: 650-467-1796; Fax: 650-467-3487; Email: salphati.laurent@gene.com

Number of text pages: 24

Number of Tables: 1

Number of Figures: 8

Number of references: 46

Number of words in Abstract: 250

Number of words in Introduction: 670

Number of words in Discussion: 1552

Nonstandard abbreviations used:

BBB, blood-brain barrier; BCRP, Breast cancer resistance protein; $Bcrp^{-/-}$, Bcrp knockout mice; %CV, coefficient of variation; DDI, drug-drug interactions; ES cells, embryonic stem cells; hBCRP, BCRP humanized mice; iv, intravenous; ITC, International Transporter Consortium; $K_{b,\ brain}$, brain-to-blood concentration ratio; PET, positron emission tomography; P-gp, P-glycoprotein; po, oral; qRT-PCR, quantitative reverse transcriptase PCR; WT, wild type.

Molecular Pharmacology Fast Forward. Published on February 18, 2016 as DOI: 10.1124/mol.115.102079
This article has not been copyedited and formatted. The final version may differ from this version.

Abstract

The breast cancer resistance protein (BCRP) is expressed in various tissues, such as the gut, liver, kidney and blood brain barrier (BBB), where it mediates the unidirectional transport of substrates to the apical/luminal side of polarized cells. Thereby BCRP acts as an efflux pump, mediating the elimination or restricting the entry of endogenous compounds or xenobiotics into tissues and it plays important roles in drug disposition, efficacy and safety. Bcrp knockout mice ($Bcrp^{-/-}$) have been used widely to study the role of this transporter in limiting intestinal absorption and brain penetration of substrate compounds. Here we describe the first generation and characterization of a mouse line humanized for BCRP (hBCRP), in which the mouse coding sequence from the start to stop codon was replaced with the corresponding human genomic region, such that the human transporter is expressed under control of the murine *Bcrp* promoter. We demonstrate robust human and loss of mouse BCRP/Bcrp mRNA and protein expression in the hBCRP mice and the absence of major compensatory changes in the expression of other genes involved in drug metabolism and disposition. Pharmacokinetic and brain distribution studies with several BCRP probe substrates confirmed the functional activity of the human transporter in these mice. Furthermore, we provide practical examples for the use of hBCRP mice to study drug-drug interactions (DDIs). The hBCRP mouse is a promising model to study the in vivo role of human BCRP in limiting absorption and BBB penetration of substrate compounds and to investigate clinically relevant DDIs involving BCRP.

Molecular Pharmacology Fast Forward. Published on February 18, 2016 as DOI: 10.1124/mol.115.102079
This article has not been copyedited and formatted. The final version may differ from this version.

Introduction

BCRP, also referred to as ABCG2, is a member of the superfamily of ATP-binding-cassette (ABC) transporters, some of which have important roles in the transport of various drugs and their metabolites (Chan et al., 2004; Leslie et al., 2005). BCRP is expressed in many different cell types, such as the luminal membrane of enterocytes, the canalicular membrane of hepatocytes, kidney proximal tubule epithelia, the luminal side of the microvascular brain endothelial cells composing the BBB, and the placenta, where it mediates the elimination and can restrict the entry of compounds into tissues (Meyer zu Schwabedissen and Kroemer, 2011). BCRP has attracted attention in drug discovery and development because of its ability to transport many commonly prescribed drugs, such as anticancer agents (e.g. topotecan, doxorubicin, methotrexate, imatinib, sorafenib or mitoxantrone), the HMG-CoA reductase inhibitor rosuvastatin, the anti-inflammatory drug sulfasalazine, the sympatholytic drug prazosin and many others (Ni et al., 2010). Furthermore, several BCRP inhibitors, such as ritonavir, omeprazole, imatinib, ivermectin, and curcumin, have been described (Jani et al., 2011; Kusuhara et al., 2012; Ni et al., 2010). Inhibition of BCRP and polymorphic variations associated with altered BCRP activity were shown to result in pharmacokinetic changes of BCRP substrates in the clinic (Hua et al., 2012; Kusuhara et al., 2012; Urquhart et al., 2008; Yamasaki et al., 2008; Zhang et al., 2006). Based on its clinical relevance, the International Transporter Consortium (ITC), followed by the FDA and EMA regulators, has recommended BCRP as one of the key transporters to be evaluated for substrate and inhibitor interactions during drug development (Giacomini et al., 2010; Zamek-Gliszczynski et al., 2012b).

Such interactions of BCRP with substrates and inhibitors are routinely tested in vitro using overexpression systems or whole cells and, theoretically, physiologically-based pharmacokinetic modelling approaches can then help to further predict complex DDIs (Rostami-Hodjegan, 2012). Despite the great value of these technologies, predicting the

Molecular Pharmacology Fast Forward. Published on February 18, 2016 as DOI: 10.1124/mol.115.102079
This article has not been copyedited and formatted. The final version may differ from this version.

effects of transporters on human pharmacokinetics and DDI potential from in vitro data alone remains challenging and preclinical in vivo studies can provide useful complementary information in this regard. Bcrp knockout mice (Jonker et al., 2002) and, more recently, rats (Zamek-Gliszczynski et al., 2012a) have helped to determine the impact of Bcrp on the pharmacokinetics and tissue distribution of various substrates, including sulfasalazine (Zaher et al., 2006; Zamek-Gliszczynski et al., 2012a), topotecan (de Vries et al., 2007), rosuvastatin (Kitamura et al., 2008), sorafenib (Lagas et al., 2010), daidzein and genistein (Enokizono et al., 2007).

However, species differences associated with this transporter may limit the use of these knockout models in predicting the role of BCRP in humans (Chu et al., 2013). While most investigations have focused on the differences in the BCRP expression level between animals and man (Chu et al., 2013; Lai, 2009; Li et al., 2009; Uchida et al., 2011; Warren et al., 2009), a few studies have also reported species differences in BCRP substrate specificity or interaction with inhibitors (Gonzalez-Lobato et al., 2010; Li et al., 2008; Mazur et al., 2012). Although the amino-acid sequences between mouse Bcrp and human BCRP are 81% identical and 86% homologous and therefore relatively conserved (Doyle and Ross, 2003), these proteins vary in more than 90 amino acids. As a single amino acid polymorphism in human BCRP can significantly alter its transport efficiency compared to the WT protein (Lee et al., 2007; Urquhart et al., 2008), differences in the kinetics of BCRP-mediated drug transport between human and mouse are very likely. Accordingly, in order to study the in vivo role of the human instead of the mouse transporter under preclinical conditions, a BCRP humanized mouse model would be of great value.

In the present work we describe the generation and extensive characterization of such a hBCRP mouse model, expressing the human in lieu of the mouse transporter under control of the murine Bcrp promoter. We determined the mRNA and protein expression, evaluated

Molecular Pharmacology Fast Forward. Published on February 18, 2016 as DOI: 10.1124/mol.115.102079
This article has not been copyedited and formatted. The final version may differ from this version.

potential compensatory changes in the expression of other genes involved in drug disposition, assessed functional activity of BCRP and conducted proof-of-concept studies for using the hBCRP mice for DDI assessment.

Molecular Pharmacology Fast Forward. Published on February 18, 2016 as DOI: 10.1124/mol.115.102079
This article has not been copyedited and formatted. The final version may differ from this version.

Materials and Methods

Chemicals and Reagents. Ultra-High Performance Liquid Chromatography (UHPLC) tandem mass spectrometry (MS/MS) protein quantification: HBSS, HEPES, Tris-HCl and sodium phosphate (Na_2HPO_4 and NaH_2PO_4) were acquired from Sigma Aldrich (Saint Quentin Fallavier, France). Reagents used for plasma membrane isolation and protein digestion, NaCl, $MgCl_2$, KCl, sucrose, EDTA, Guanidine-HCl, DTT, iodoacetamide, bovine serum albumin (BSA), dextran (molecular weight 70.000) and urea also came from Sigma Aldrich (Saint Quentin Fallavier, France). The complete Mini (EDTA-free) Protease Inhibitor Cocktail tablets were purchased from Roche (Bâle, Switzerland). Chloroform (HiPerSolv, Chromanorm for HPLC) was supplied by VWR (Strasbourg, France). HPLC-grade acetonitrile and methanol were purchased at Merck (Nogent-sur-Marne, France). Formic acid (99% w/w), HPLC grade, was supplied by Fischer Scientific (Illkirch, France). All the water was prepared with a Milli-Q water purification system (Millipore, Molsheim, France). Sequencing grade Modified Trypsin, Mass Spectrometry grade rLys-C and ProteaseMAX surfactant were from Promega (Charbonnières-les-Bains, France). The measurement of protein concentration was carried out by using the Micro BCA Protein Assay Kit (Thermo Scientific, Illkirch, France). Standard solutions of peptides were provided by Pr. M. Vidal and Dr. W. Q. Liu (UMR 8638, Chimie organique médicinale et extractive - Toxicologie expérimentale) or by Pepscan (Lelystad, The Netherlands). The accurate concentration of each standard solution was determined, after acid hydrolysis and amino-acid analysis by Dr. E. Thioulouse (Laboratoire de Biochimie, Hôpital Trousseau, Paris, France) or by Pepscan (Lelystad, The Netherlands).

Sulfasalazine/Ko143 interaction, daidzein, genistein, rosuvastatin and topotecan in vivo studies: Sulfazalasine, daidzein, genistein and topotecan were purchased from Sigma-Aldrich (St. Louis, MO) and Ko143 from Enzo Life Sciences (Plymouth Meeting, PA). Rosuvastatin

Molecular Pharmacology Fast Forward. Published on February 18, 2016 as DOI: 10.1124/mol.115.102079
This article has not been copyedited and formatted. The final version may differ from this version.

was obtained from TSZ Chem (Framingham, MA). 1-methyl-2-pyrrolidone (NMP), Solutol (Kolliphor HS 15), thenyoltrifluoroacetone (TTFA), DMSO and Tween20 were obtained from Sigma-Alrich (St. Louis, MO). Saline was obtained from Baxter (Deerfield, IL). Ammonium acetate and glacial acetic acid were obtained from Fisher Scientific (Waltham, MA).

Positron emission tomography (PET) study: Tariquidar dimesylate and Ko143 for the PET study were obtained from Xenova Ltd. (Slough, UK) and Axon Medchem BV (Groningen, The Netherlands), respectively.

Generation of hBCRP and Bcrp$^{-/-}$ mice. hBCRP and Bcrp$^{-/-}$ mice were generated by Taconic Biosciences GmbH (Cologne, Germany) as described below. DNA constructs and cloning: For targeting the *Bcrp* gene locus basic vectors containing (1) neomycin and puromycin expression cassettes flanked by *frt* and *f3* sites, respectively, (2) a ~5 kb genomic sequence upstream of the translational start ATG of the mouse *Bcrp* gene on exon 2 and a ~7 kb genomic sequence downstream of the stop codon on exon 16 used as targeting arms for homologous recombination have been constructed. The final targeting vector shown in Fig. 1B was generated by fusing a genomic fragment from start ATG to stop codon of human *BCRP* in frame to the aforementioned targeting arms by subcloning the fragments via consecutive red/ET recombineering (Zhang et al., 1998) into the bacterial artificial chromosome RP11-183N11 (Source BioScience, Nottingham, United Kingdom) containing the genomic sequence of human *BCRP*. The coding exons 2-16 from this clone were sequences and confirmed to match the human BCRP reference sequence (http://www.uniprot.org/uniprot/Q9UNQ0).

Generation and molecular characterization of targeted embryonic stem cells: Culture and targeted mutagenesis of embryonic stem (ES cells) were carried out as described previously (Behringer et al., 2014). The targeting vector was linearized with *Not*I and electroporated into a C57BL/6NTac mouse ES cell line. Of 256 G418 and puromycin resistant ES cell colonies screened by standard Southern blot analyses, 14 correctly targeted clones were identified, 4 of

Molecular Pharmacology Fast Forward. Published on February 18, 2016 as DOI: 10.1124/mol.115.102079
This article has not been copyedited and formatted. The final version may differ from this version.

which were expanded and further analysed by Southern blot analyses with 5' and 3' external probes and internal probes. All of these clones were confirmed as correctly targeted at both homology arms without additional random integrations (data not shown).

Generation and molecular characterization of hBCRP and Bcrp$^{-/-}$ mice: For the generation of hBCRP mice, 3 correctly targeted ES cell clones were expanded, injected into BALBc-blastocysts and transferred into foster mothers as described previously (Behringer et al., 2014). Litters from these fosters were inspected visually and chimerism was determined by hair colour. Highly chimeric animals obtained from one of the 3 correctly targeted clones were used for breeding to an efficient flipase (Flpe) deleter strain carrying a transgene that expresses Flpe in the germ line in order to delete the neomycin and puromycin expression cassettes in the offspring (Fig. 1D). Offspring from these crosses were analysed by PCR in order to identify heterozygous *BCRP* humanized mice. These heterozygous mice were either crossed with each other to generate homozygous hBCRP mice or crossed to a deleter strain carrying a transgene that expresses Cre-recombinase in the germ line in order to delete the human *BCRP* exons 3-15 (Fig. 1E). Offspring from the latter crosses were analysed by PCR in order to identify heterozygous *Bcrp* knockout mice, which were then further crossed to generate homozygous Bcrp$^{-/-}$ mice. The Flpe- and Cre-deleter strains mentioned above were generated in house on a C57BL/6NTac genetic background.

Animal husbandry and experimentation. hBCRP and Bcrp$^{-/-}$ mice were bred at Taconic Biosciences GmbH (Cologne, Germany) to obtain homozygous age-matched mice and age- and sex-matched C57BL/6NTac wild type (WT) controls were obtained from Taconic Biosciences, Inc. (Hudson, NY). These three mouse lines are maintained and available through Taconic Biosciences. Animals were allowed to acclimatize for at least five days prior to an experimental procedure at all experimental locations. Mice were kept in agreement with local laws and regulations and in temperature-controlled environments with 12-hour light cycles and given standard diets and water ad libitum. All animal procedures were approved by

Molecular Pharmacology Fast Forward. Published on February 18, 2016 as DOI: 10.1124/mol.115.102079
This article has not been copyedited and formatted. The final version may differ from this version.

local Institutional Animal Care and Use Committees.

Quantitative Reverse Transcriptase PCR (qRT-PCR). Details on the preparation of mRNA, the synthesis of cDNA, the primers used and the methods of data analysis for qRT-PCR are provided in the Supplemental Materials and Methods.

Affymetrix expression profiling (Microarray Analysis). Details on the preparation of mRNA, quality and quantity determination, cDNA synthesis, used GeneChip Array and data processing methods are provided in the Supplemental Materials and Methods.

Cortical microvessel isolation, preparation of plasma membrane fraction from different tissues, protein digestion and quantification by UHPLC MS/MS. Details on the isolation of brain microvessels, preparation of plasma membrane fraction from microvessels, liver and kidney, protein digestion and quantification by UHPLC MS/MS are provided in the Supplemental Materials and Methods.

Sulfasalazine, daidzein, genistein, rosuvastatin and topotecan in vivo studies. Details on the sulfasalazine, daidzein. genistein, rosuvastatin and topotecan pharmacokinetics studies and the sulfasalazine/Ko143 interaction study and corresponding LC-MS/MS and pharmacokinetic analyses are provided in the Supplemental Materials and Methods.

PET study. Details on general procedures, animal handling, PET imaging, metabolite analysis and statistical analysis are provided in the Supplemental Materials and Methods.

Statistical analysis. Student's t-test or one-way ANOVA were applied to determine statistical significances in differences between WT, Bcrp$^{-/-}$ and hBCRP mice. Values were considered statistically different when $p<0.05$. Analyses were done using Microsoft Excel or GraphPad Prism 5.

Molecular Pharmacology Fast Forward. Published on February 18, 2016 as DOI: 10.1124/mol.115.102079
This article has not been copyedited and formatted. The final version may differ from this version.

Results

Generation of hBCRP and Bcrp$^{-/-}$ mice. hBCRP mice were generated by a knock-in strategy as depicted in Fig. 1, such that the coding sequence of mouse Bcrp from its start codon on exon 2 to its stop codon on exon 16 was replaced by the corresponding genomic human region in mouse ES cells (Fig. 1A-D). As a result of this approach the human instead of mouse transporter is expressed under control of the mouse Bcrp promoter. Transgenic mice were generated from correctly targeted ES cells. The neomycin and puromycin expression cassettes used for ES cell clone selection were deleted via Flp-recombinase mediated recombination in vivo by crossing hBCRP transgenic mice with a mouse line expressing Flp-recombinase in the germ line (Fig. 1D). Functional inactivation of the BCRP gene was achieved by crossing hBCRP mice with a mouse line expressing Cre-recombinase in the germ line resulting in a deletion of human BCRP exons 3-15 (Fig. 1E). Homozygous hBCRP and Bcrp$^{-/-}$ mice obtained by breeding appeared normal, could not be distinguished from WT animals, and had normal survival rates and fertility.

Human *BCRP* and mouse *Bcrp* mRNA expression in WT, hBCRP and Bcrp$^{-/-}$ mice. In order to confirm expression of human *BCRP* mRNA in different tissues of the hBCRP mice, a TaqMan analysis was conducted on liver, kidney, duodenum, ileum, jejunum, colon, heart, lung, testis and whole brain samples of WT, hBCRP and Bcrp$^{-/-}$ male and female mice, using a mouse Bcrp and a human BCRP specific TaqMan assay (n=3 mice per sex and genotype). The human *BCRP* mRNA was detectable in all tissues of the hBCRP mice, but not in WT or Bcrp$^{-/-}$ animals. Based on Ct values the highest expression was observed in the kidney, followed by ileum, duodenum and jejunum, colon, testis, liver, brain, lung and heart (Supplemental Table 1). The same pattern of expression was observed for mouse *Bcrp* in WT mice, when a murine specific *Bcrp* TaqMan assay was used (Supplemental Table 1). Compared to murine *Bcrp* mRNA in WT animals, human *BCRP* in the hBCRP mice was

Molecular Pharmacology Fast Forward. Published on February 18, 2016 as DOI: 10.1124/mol.115.102079
This article has not been copyedited and formatted. The final version may differ from this version.

expressed at slightly lower levels, with some variability between organs. While the *Bcrp*/*BCRP* expression in the brain was almost identical between WT and hBCRP mice, the human *BCRP* expression in the kidney and the testis of the hBCRP mice was only ~30% of the murine *Bcrp* expression in the WT. All other values varied between these two extremes (Fig. 2). In general the expression level of mouse *Bcrp* in WT animals was similar between both sexes for most organs, except in the liver where it was 2.5-fold lower and in the duodenum and ileum where it as ~1.5-fold higher in females compared to males. The hBCRP mice showed the same difference in human *BCRP* expression between males and females for the liver and the ileum, while the level was identical between both sexes in the duodenum (Fig. 2, Supplemental Table 1). In summary, a robust expression of human *BCRP* mRNA in absence of mouse *Bcrp* mRNA expression was observed in hBCRP mice. The differences in relative expression levels between organs were the same as that of mouse *Bcrp* in WT mice with similar variations between males and females, albeit the human transcript was expressed at slightly lower levels than its mouse orthologue.

Bcrp/BCRP protein quantification in WT and hBCRP mice. Bcrp/BCRP protein amounts in WT and hBCRP mice were determined in kidney (n=3 mice per strain), liver (n=3 mice per strain) and cortical brain vessels (n=2 mice for WT and n=3 mice for hBCRP) by UHPLC MS/MS analysis using peptides specific to human BCRP, or to mouse Bcrp, and additionally peptides that are in common to both mouse and human Bcrp/BCRP (Supplemental Table 2). The plasma membrane marker Na^+/K^+ ATPase was used as a control to evaluate the extraction and digestion homogeneity between each tissue samples, as previously proposed (Hoshi et al., 2013). The homogeneity of liver and kidney samples was confirmed by the low variability of Na^+/K^+ ATPase amounts with coefficients of variation (%CV) of 8.9 and 24.9% in WT mice and 8.6 and 13.6% in hBCRP mice, respectively (Table 1). Cortical vessels were less homogenous due to the low protein amounts available for the assay of each sample (%CV

Molecular Pharmacology Fast Forward. Published on February 18, 2016 as DOI: 10.1124/mol.115.102079
This article has not been copyedited and formatted. The final version may differ from this version.

= 31.9% in WT and 32.9% in hBCRP mice). No significant differences in Na^+/K^+ ATPase expression levels were observed in any sample between WT and hBCRP mice (Table 1).

The peptide specific to human BCRP was detected in all samples of hBCRP but not WT mice, while the opposite was the case for the mouse Bcrp-specific peptide (data not shown). For direct comparison of protein amounts between WT and hBCRP mice we used the data obtained with the common Bcrp/BCRP peptide (Table 1). Consistent with the mRNA analysis, the highest Bcrp/BCRP protein expression was observed in kidney (WT = 37.7, hBCRP = 9.34 fmol/µg of protein), followed by liver (WT = 1.55, hBCRP = 0.73 fmol/µg of protein) and brain cortical vessels (WT = 0.23, hBCRP = 0.39 fmol/µg of protein). The average Bcrp/BCRP protein amount in hBCRP mice was 4-fold lower in kidney ($p < 0.001$), 2.1-fold lower in liver ($p < 0.001$) and 1.7-fold higher in brain vessels (statistically not significant) compared to WT controls, which overall is in reasonable agreement with the mRNA measurements.

Assessment of hepatic gene expression changes in Bcrp$^{-/-}$ and hBCRP mice. Potential compensatory gene expression changes in liver of Bcrp$^{-/-}$ and hBCRP mice relative to WT controls were assessed by microarray analysis. The comparison between Bcrp$^{-/-}$ and WT mice revealed a total of 22 unique genes (24 total, including genes that are duplicated within the array) altered by greater than 2-fold ($p < 0.05$) (Supplemental Table 3). As expected, the hepatic expression of mouse *Bcrp* was most significantly suppressed compared to WT controls (87-fold decrease). Other expression changes in genes coding for proteins (potentially) involved in drug metabolism and disposition were observed for monooxygenase DBH-like (*Moxd*) 1 (17.6-fold increase in Bcrp$^{-/-}$ compared to WT mice), solute carrier 3a1 and 41a2 (2.1 and 2.0-fold increase, respectively) and the cytochrome P450 isoform 2b10 (3-fold decrease). In addition, significant changes were noted in some genes not involved in drug metabolism and disposition, such as lipocalin 2, orosomucoid 2 (which can be involved in

Molecular Pharmacology Fast Forward. Published on February 18, 2016 as DOI: 10.1124/mol.115.102079
This article has not been copyedited and formatted. The final version may differ from this version.

plasma protein binding of certain drugs (Silamut et al., 1991)), metallothionein 2, and serum amyloid A3 (8.6, 4.9. 4.7 and 4.2-fold increase, respectively). Relative comparison of hBCRP to WT mice detected 4 genes as significantly changed. In addition to the 78-fold decrease of hepatic *Bcrp*, an 8.7-fold increase of *Moxd1* expression was the only change of genes coding for proteins involved in drug metabolism and disposition. Additionally, serpine 2 was increased by 2.6-fold and the transmembrane protein 223 was decreased by 2.6-fold (Supplemental Table 3).

Concentration of sulfasalazine, daidzein, genistein, rosuvastatin and topotecan in blood and other tissues of WT, hBCRP and Bcrp$^{-/-}$ mice. The expression of functional BCRP in hBCRP mice was assessed by comparing the concentration-time profiles of various BCRP probe substrates in blood and different tissues of WT, hBCRP and Bcrp$^{-/-}$ mice.

Sulfasalazine: Following 5 mg/kg intravenous (iv) or 20 mg/kg oral (po) administration of sulfasalazine, blood concentrations were markedly higher in Bcrp$^{-/-}$ than in WT and hBCRP mice (Fig. 3A and B). In WT mice, blood concentrations were below the limit of quantitation after 2 and 1 hour, for the iv and po dose, respectively. Consequently, PK analyses and comparisons of WT animals with the two other strains were performed with parameters calculated using concentrations up to 1 or 2 hours (Supplemental Table 4A), as well as based on the complete profiles (up to 6 hours; Supplemental Table 4B) from the other strains.

Blood exposure to sulfasalazine was significantly ($p<0.05$) increased in Bcrp$^{-/-}$ compared to WT mice after iv (8.3-fold) and po (117-fold) administration (Supplemental Table 4A). Concentrations (and profiles) in hBCRP mice were intermediate between those observed in the WT and Bcrp$^{-/-}$ mice (Figs. 3A and B), with concentrations measurable up to 6 hours. This was reflected by a modest 2.7- fold higher AUC_{0-2} in humanized compared to WT mice following iv dosing and 4.6- fold higher AUC_{0-1} after po administration. Importantly, sulfasalazine exposure in hBCRP mice was nevertheless significantly ($p<0.05$) lower than in

Molecular Pharmacology Fast Forward. Published on February 18, 2016 as DOI: 10.1124/mol.115.102079
This article has not been copyedited and formatted. The final version may differ from this version.

Bcrp$^{-/-}$ animals (Supplemental Tables 4A and B) after dosing through either route. Clearance in Bcrp$^{-/-}$ mice was 8.4-fold lower than in WT controls, while in hBCRP mice, it was only decreased by 2.7-fold.

Daidzein: The plasma concentration of daidzein was slightly increased in Bcrp$^{-/-}$ compared to WT mice over a period of one hour after administration of a 5 mg/kg iv dose, with a significant 1.5-fold higher plasma concentration at the earliest measured time point (5 minutes after administration). In contrast, the concentration-time profiles in hBCRP and WT mice were comparable (Fig. 4A, B). The mean brain concentrations of daidzein were significantly higher in Bcrp$^{-/-}$ compared to WT mice at 0.5, 1 and 2 hrs after administration, but comparable between WT and hBCRP animals (Figure 4C-E). Namely, at the 0.5 hrs time point the daidzein mean brain concentration was increased by ~4.7-fold in Bcrp$^{-/-}$ compared to WT and hBCRP mice (Fig. 4C). This difference is also reflected by the significantly higher brain-to-plasma concentration ratio in Bcrp$^{-/-}$ mice (1.13) relative to WT (0.20) and hBCRP (0.11) animals. At the 1 and 2 hr time points daidzein was below the limit of quantification in brain tissue of WT and hBCRP mice, but still detectable in Bcrp$^{-/-}$ mice (Fig. 4D and E).

Genistein: The blood concentration of genistein was higher in Bcrp$^{-/-}$ compared to WT mice (Fig. 5A-C), with statistically significant 2.2- and 2.2-fold increases in $AUC_{0\text{-}24hrs}$ following 20 mg/kg iv and 50 mg/kg po administration, respectively (Supplemental Table 5). Furthermore, the $AUC_{0\text{-}6hrs}$ was 2.0-fold higher in Bcrp$^{-/-}$ mice receiving a 20 mg/kg po dose of genistein, while the blood clearance in these mice after 20 mg/kg iv administration was 2.4-fold lower relative to the WT controls (Supplemental Table 5). The Bcrp$^{-/-}$ animals also showed a statistically significant 1.5-fold higher $AUC_{0\text{-}6hrs}$ and $AUC_{0\text{-}24hrs}$ following 20 and 50 mg/kg po doses of genistein compared to hBCRP mice (Supplemental Table 5). Brain concentrations were analysed 15 and 90 min after 20 mg/kg iv administration of genistein. Bcrp$^{-/-}$ mice showed significantly higher brain concentrations than WT and hBCRP animals at both time points, with 2.6 and 4.4-fold increases at 15 min and 8.1 and 9.9-fold increases at

Molecular Pharmacology Fast Forward. Published on February 18, 2016 as DOI: 10.1124/mol.115.102079
This article has not been copyedited and formatted. The final version may differ from this version.

90 min compared to WT and hBCRP mice, respectively (Fig. 5D and E). Furthermore, the brain-to-blood concentration ratio ($K_{b,\ brain}$) values in Bcrp$^{-/-}$ mice were 3.3 and 5.1-fold higher at 15 min and 19.0 and 7.6-fold higher at 90 min than in WT and hBCRP animals (Fig. 5F). Genistein concentrations were also measured in testis, liver and kidney following 20 mg/kg iv administration, but most differences between WT, Bcrp$^{-/-}$ and hBCRP mice were not significant (data not shown).

Rosuvastatin: Bcrp$^{-/-}$ mice showed statistically significant higher blood concentrations of rosuvastatin compared to WT controls following 6.1 mg/kg iv and 13.7 mg/kg po administration (Fig. 6A, B), as reflected by 4.2 and 3.1-fold $AUC_{0\text{-}24hrs}$ and 1.7 and 6.7-fold increases in C_{max} at these doses, respectively (Supplemental Table 6). In contrast, hBCRP mice showed no statistically significant difference in rosuvastatin blood concentrations to WT animals after iv administration and only marginal and statistically insignificant 1.6 and 1.7-fold increases in $AUC_{0\text{-}24hrs}$ and C_{max} following oral administration (Fig. 6A, B, Supplemental Table 6). Brain, kidney and liver concentrations were also measured at 15 min and 1 h after po administration, but due to the small number of animals and high variability between individual mice from each group no significant changes were observed between the different lines (data not shown). The % recovery of parent compound in feces and urine after iv administration and in urine after oral administration of rosuvastatin was highest in WT and lowest in Bcrp$^{-/-}$ mice, with hBCRP animals in between (Supplemental Table 7).

Topotecan: Following 1 mg/kg iv and po administration the topotecan blood concentrations in Bcrp$^{-/-}$ mice were higher compared to WT controls (Fig. 7A and B), with concomitant significant 6.1-fold increases in $AUC_{0\text{-}4h}$ after po dosing (Supplemental Table 8). Blood concentrations in hBCRP mice were between these two lines (Fig. 7A and B), showing a significant 1.5-fold lower $AUC_{0\text{-}4h}$ than Bcrp$^{-/-}$ mice after po administration (Supplemental Table 8). Compared to WT animals the clearance after iv administration was 1.6 and 1.4-fold lower in Bcrp$^{-/-}$ and hBCRP mice, respectively. Following po administration the C_{max} in Bcrp^{-}

Molecular Pharmacology Fast Forward. Published on February 18, 2016 as DOI: 10.1124/mol.115.102079
This article has not been copyedited and formatted. The final version may differ from this version.

$^{/-}$ mice was increased by 5.6 and 1.7-fold relative to WT and hBCRP animals, respectively (Supplemental Table 8). While no significant differences were observed between the three lines in topotecan brain exposure 15 minutes after 1 mg/kg po administration (Fig. 7C), brain concentrations were moderately, but statistically significantly increased by 3.1 and 1.7-fold after 60 minutes in Bcrp$^{-/-}$ mice compared to WT and hBCRP animals, respectively (Fig. 7D). As a consequence of the lower topotecan blood concentrations in WT mice, $K_{b,\ brain}$ values were higher relative to Bcrp$^{-/-}$ and hBCRP mice at both time points (Fig. 7E).

BCRP inhibition studies related to oral bioavailability of sulfasalazine and brain penetration of tariquidar. The possibility of inhibiting intestinal BCRP activity was tested by treating WT, Bcrp$^{-/-}$ and hBCRP mice with a 20 mg/kg po dose of Ko143 30 minutes prior to the administration of 20 mg/kg po sulfasalazine. No significant changes in sulfasalazine blood concentrations, $AUC_{0\text{-last}}$ and C_{max} were observed in Ko143 pre-treated relative to untreated Bcrp$^{-/-}$ mice (Fig. 3C, Supplemental Table 4B). In contrast, pre-treatment with Ko143 increased the blood concentrations of sulfasalazine in WT and hBCRP mice (Fig. 3C), detectable up to 6 hours post-dose. This was associated with significant 25.8 and 6.5-fold increases in $AUC_{0\text{-}1}$ and 45.6 and 5.3-fold increases in $AUC_{0\text{-last}}$ in WT and hBCRP mice, respectively (Supplemental Table 4A and B). Although C_{max} in WT mice under control conditions could only be estimated from three timepoints, it was significantly increased from 0.25 µM to 5.36 µM with Ko143. Similarly, C_{max} in hBCRP mice was 5-2-fold greater in the presence of Ko143 (Supplemental Table 4B).

We also assessed the functional activity of BCRP/Bcrp and its inhibition at the BBB of hBCRP and WT mice in vivo using positron emission tomography (PET) and [^{11}C]tariquidar as radiotracer, which is a metabolically stable substrate of murine and human P-glycoprotein (P-gp) as well as murine Bcrp and human BCRP (Bankstahl et al., 2013; Kannan et al., 2011). We have shown before that [^{11}C]tariquidar can be used to visualize Bcrp functional activity at the murine BBB when used at P-gp-saturating tariquidar plasma concentration levels (Wanek

Molecular Pharmacology Fast Forward. Published on February 18, 2016 as DOI: 10.1124/mol.115.102079
This article has not been copyedited and formatted. The final version may differ from this version.

et al., 2012). Mice underwent [^{11}C]tariquidar PET scans after (i) pretreatment with vehicle only, (ii) pretreatment with unlabelled tariquidar at a dose of 12 mg/kg which inhibits P-gp at the BBB without inhibiting BCRP/Bcrp and (iii) pretreatment with tariquidar (12 mg/kg) and the BCRP/Bcrp inhibitor Ko143 (10 mg/kg) (Allen et al., 2002) as described previously (Wanek et al., 2012) (Fig. 8). We assessed radiolabelled metabolites of [^{11}C]tariquidar in plasma and brain samples collected at the end of PET scanning by radio-TLC analysis. At 60 minutes after [^{11}C]tariquidar injection 80 ± 14% (n = 12) and 85 ± 12% (n = 11) of radioactivity in plasma and 93 ± 8% (n = 6) and 97 ± 2% (n = 3) in brain was in the form of unchanged [^{11}C]tariquidar for hBCRP and WT mice, respectively. This suggested that there were no differences in radiotracer metabolism between hBCRP and WT mice. Brain uptake of [^{11}C]tariquidar was expressed as $K_{b,brain}$ of radioactivity in the last PET frame (i.e. at 50-60 minutes after radiotracer injection). In vehicle scans, $K_{b,brain}$ values were low and not significantly different between hBCRP and WT mice ($K_{b,brain}$ (mean ± SD) hBCRP: 1.58 ± 0.38; WT: 1.50 ± 0.25), which was consistent with restriction of brain distribution of [^{11}C]tariquidar by P-gp and BCRP/Bcrp. In scans after P-gp inhibition with tariquidar (12 mg/kg), $K_{b,brain}$ values were only moderately and not significantly increased as compared with vehicle treated animals in hBCRP mice ($K_{b,brain}$: 3.20 ± 0.21, 2.0-fold increase) and WT mice ($K_{b,brain}$: 3.35 ± 0.31, 2.2-fold increase), which was consistent with functional compensation of P-gp inhibition by BCRP/Bcrp for dual P-gp/BCRP substrates (Kodaira et al., 2010). In scans after P-gp and BCRP/Bcrp inhibition with tariquidar (12 mg/kg) and Ko143 (10 mg/kg), respectively, $K_{b,brain}$ values were significantly (P<0.001, 1-way ANOVA followed by Bonferroni´s multiple comparison test) increased as compared with tariquidar only treated animals by 3.6-fold in hBCRP mice ($K_{b,brain}$: 11.66 ± 2.16) and by 3.3-fold in WT mice ($K_{b,brain}$: 10.90 ± 0.93). This strongly suggested that hBCRP and WT mice had comparable functional activity of BCRP/Bcrp at the BBB and that this transporter was effectively inhibited by Ko143.

Molecular Pharmacology Fast Forward. Published on February 18, 2016 as DOI: 10.1124/mol.115.102079
This article has not been copyedited and formatted. The final version may differ from this version.

Discussion

Here, we describe the generation of a humanized BCRP mouse model via a sophisticated replacement of the murine *Bcrp* coding sequence with corresponding human genomic DNA, such that the human transporter is expressed under control of the mouse *Bcrp* promoter (Fig. 1). The hBCRP mice were healthy and showed no obvious phenotypic abnormalities. Human *BCRP* mRNA was detected in the expected organs, such as liver, gut, brain, kidney and testis of humanized mice, albeit at slightly lower levels than mouse *Bcrp* mRNA in WT mice in most tissues (Fig. 2). The mRNA measurement were further confirmed by protein quantification in selected organs, showing the BCRP amounts to be 2 and 4-fold lower in liver and kidney, respectively, and 1.7-fold higher (not statistically significant) in cortical vessels of hBCRP compared to WT mice (Table 1).

Although the hepatic and renal protein amounts of Bcrp and Na^+/K^+ ATPase in membrane fractions are within the same magnitude as previously reported by Kamiie et al. using similar extraction methods on tissues from a ddy WT mouse strain (Kamiie et al., 2008), we observed lower Bcrp levels in the C57BL/6NTac mice used in our study (1.55 vs 8.84 fmol/µg of protein). The most likely explanation for this is an inter-strain difference. When comparing our results for cortical vessels with those previously described in C57BL/6 mice by Sadiq et al. (Sadiq et al., 2015), we measured significantly lower levels in this tissue (0.225 fmol/µg vs 8.69 fmol/µg of protein). However, the method of vessel isolation differed between the two studies, such that Sadiq et al. obtained capillaries from whole brain lysate and carried out three successive filtrations (210, 85 and 20 µm nylon mesh) in order to enrich in microcapillaires, whereas we used only one 10 µm nylon mesh to filter cortical vessels. Therefore, the lower values can be explained by a dilution of Bcrp/BCRP in our samples. Taking into account that the average BCRP/Bcrp protein amount in the human BBB was

Molecular Pharmacology Fast Forward. Published on February 18, 2016 as DOI: 10.1124/mol.115.102079
This article has not been copyedited and formatted. The final version may differ from this version.

recently shown to be 1.85-fold greater than in WT mice (Uchida et al., 2011) and that we observed a 1.75-fold higher expression level of human BCRP in cortical vessels of hBCRP mice than murine Bcrp in WT controls (Table 1), we conclude that the expression level of this transporter in hBCRP mice and humans is similar. The comparison of BCRP protein levels between humans and hBCRP mice in other organs requires further investigation.

No compensatory changes in the expression of genes coding for proteins involved in drug metabolism and disposition were observed in liver of hBCRP mice compared to WT controls with the exception of an 8.7-fold increase of *Moxd1* mRNA (Supplemental Table 3). The presumably very minor role of Moxd1 in drug metabolism and disposition (Chambers et al., 1998) and the moderate (2.6-fold) change of only two other genes, serpine 2 and transmembrane protein 223, in hBCRP mice, are not expected to limit their use to study BCRP-mediated absorption or disposition. Of the expression changes in 22 genes in $Bcrp^{-/-}$ mice only a ~2-fold increase in solute carriers 3a1 and 41a2, which don't appear to play relevant roles in drug transport, and 3-fold decrease in the cytochrome P450 isoform 2b10 expression are of potential interest in the context of drug metabolism and disposition (Supplemental Table 3), but these changes do not preclude the general application of these mice. Further investigations will be needed to assess changes in other tissues.

Our studies confirmed the important role of Bcrp/BCRP in oral bioavailability and/or tissue distribution of sulfasalazine, daidzein, genistein, rosuvastatin and topotecan, as demonstrated by the various differences in pharmacokinetics and brain penetration of these compounds between WT, hBCRP and $Bcrp^{-/-}$ mice. Moreover, the functional activity of human BCRP in hBCRP mice was clearly shown by comparing the blood and tissue exposure of these BCRP probe substrates between the three mouse lines. In the case of sulfasalazine, the AUC after iv and po administration was increased significantly more in $Bcrp^{-/-}$ than in hBCRP mice when compared to WT controls (Supplemental Table 4A). In addition, the clearance and C_{max} of sulfasalazine were altered to a much lesser extent in hBCRP than in $Bcrp^{-/-}$ mice. Similar

Molecular Pharmacology Fast Forward. Published on February 18, 2016 as DOI: 10.1124/mol.115.102079
This article has not been copyedited and formatted. The final version may differ from this version.

observations were made for the plasma or blood concentrations of daidzein (Fig. 4A, B), genistein (Fig. 5A-C) and rosuvastatin (Fig. 6A, B, Supplemental Table 6), which were slightly increased in Bcrp$^{-/-}$ but not hBCRP mice relative to WT controls. Furthermore, the mean brain concentration and brain-to-plasma ratio of daidzein and genistein were significantly higher in Bcrp$^{-/-}$ compared to WT and hBCRP animals (Fig. 4C-E, Fig. 5D-F). Blood concentrations of topotecan in hBCRP mice after iv and po administration as well as brain concentrations 60 minutes after po dosing were also lower compared to Bcrp$^{-/-}$ animals, but the recovery towards WT levels was relatively weak (Fig. 7A, B, D, Supplemental Table 8). Based on our results the overall relevance of Bcrp/BCRP in restricting the brain penetration of the dual P-gp/BCRP substrate topotecan appears to be relatively low, which is in agreement with a previous study (de Vries et al., 2007) and can be attributed to the activity of P-gp compensating the loss of Bcrp. Accordingly, the higher $K_{b,\ brain}$ values at 15 and 60 minutes after po administration in WT compared to Bcrp$^{-/-}$ and hBCRP mice (Fig. 7E) are a consequence of the lower topotecan blood concentrations in WT mice, i.e. the relatively stronger effect of Bcrp in limiting oral bioavailability versus brain penetration. In summary, our data demonstrate that human BCRP is able to functionally compensate for the loss of mouse Bcrp in the hBCRP mice.

A consistent trend observed for all five probe substrates is that the blood concentrations in hBCRP mice never reach the levels observed in WT controls. This observation might be generally explained by the lower expression level of the transporter in the gut, liver and kidney of the humanized mice (Fig. 2), though species differences in the transport activity between murine Bcrp and human BCRP might contribute to this result for some of the compounds. The latter point might also explain why the pharmacokinetic profiles of sulfasalazine, rosuvastatin and topotecan in hBCRP mice vary in different ways from those observed in WT and Bcrp$^{-/-}$ mice. Furthermore, we cannot exclude that changes in the expression level of other transporters or drug metabolizing enzymes contribute to the

Molecular Pharmacology Fast Forward. Published on February 18, 2016 as DOI: 10.1124/mol.115.102079
This article has not been copyedited and formatted. The final version may differ from this version.

differences in the pharmacokinetic profiles in the hBCRP mice. However, based on the results from our microarray studies (Supplemental Table 3) such changes appear to be minimal and they are unlikely to be of major relevance. In contrast to the results observed for blood concentrations, daidzein and genistein brain concentrations were fully recovered (Fig. 4C-E, Fig. 5D-F), consistent with the similar expression level of Bcrp/BCRP in cortical vessels of WT and hBCRP mice (Fig. 2, Table 1). Interestingly, the topotecan brain concentration in hBCRP mice was 1.8-fold higher ($P<0.05$) than in WT mice 60 minutes after po administration (Fig. 7D). This observation might be attributed to a species difference in the topotecan transport activity of mouse Bcrp versus human BCRP, which could also explain the relatively weak recovery of blood concentrations in hBCRP mice (Fig 7A and B).

In addition to assessing substrate interactions with BCRP, studying DDIs caused by the inhibition of this transporter is a potentially valuable application of the hBCRP mice. In order to evaluate their utility for this type of application, we investigated the effect of the BCRP inhibitor Ko143 on oral bioavailability of sulfasalazine and brain penetration of tariquidar. Ko143 increased the blood concentrations, $AUC_{0\text{-}last}$ (and $AUC_{0\text{-}1}$) and C_{max} of sulfasalazine in WT and hBCRP but not $Bcrp^{-/-}$ animals (Fig. 3C, Supplemental Tables 4A and B), whereby the stronger inhibitory effect in WT compared to hBCRP mice might be attributed to the differences in the expression level of Bcrp/BCRP in the gut of these the two mouse lines. In agreement with the comparable expression level of Bcrp/BCRP at the BBB in WT and hBCRP mice, Ko143 increased the $K_{b,brain}$ value of tariquidar to a similar extent in both lines (Fig. 8E).

The present work describes the first generation and extensive characterization of a humanized BCRP mouse model. The results from these studies demonstrate the integrity and functionality of this novel model. The hBCRP mouse provides a valuable alternative or adjunct to WT animals in studies using Bcrp knockout mice or chemical inhibitors of

Molecular Pharmacology Fast Forward. Published on February 18, 2016 as DOI: 10.1124/mol.115.102079
This article has not been copyedited and formatted. The final version may differ from this version.

BCRP/Bcrp aiming to assess substrate or inhibitor in vivo interactions with BCRP, specifically where species differences are of concern. Though the results obtained with topotecan might indicate a difference in the topotecan transport activity of mouse Bcrp versus human BCRP (see above), the systematic analysis of species differences by using the hBCRP mice is beyond the scope of this work and will be subject to further investigations. Based on previously published work, fumitremorgin C could be considered as a potential inhibitor (Gonzalez-Lobato et al., 2010) and pheophorbide A or bisphenol A as substrates (2010; Li et al., 2008; Mazur et al., 2012) for such studies. Thus, the hBCRP mouse model provides a novel tool for identifying differences in inhibitor or substrate interactions with this transporter, either for basic research purposes or in drug development. With regards to the latter, this information, in conjunction with results obtained from in vitro studies and in Bcrp$^{-/-}$ mice, can help to estimate the potential need for clinical DDI studies.

Molecular Pharmacology Fast Forward. Published on February 18, 2016 as DOI: 10.1124/mol.115.102079
This article has not been copyedited and formatted. The final version may differ from this version.

Acknowledgements

We wish to thank Heidrun Kern and Steffen Guettler from Taconic Biosciences GmbH, Aysel Gueler, Ina Mairhofer and Klaus Magin from Abbvie, William Kintigh, Manna Manna, Christine Stewart, Stephen O'Sullivan (in vivo group) and Monica Singer from Janssen, Scott Fauty, Karen Owens, Gino Salituro from Merck Sharp & Dohme, the GlaxoSminthKline DMPK, Laboratory Animal Services and Statistics departments (Caroline Sychterz, JoAnn Coleman, Debra Paul, Edward Long, Deborah McCoy, Holly Sekellick and Leonard Azzarano), Meryam Taghi from Université Paris Descartes and the In Vivo Studies Group at Genentech for excellent technical assistance. We want to acknowledge Cerina Chhuon and Chiara Guerrera (Proteomic Platform Necker, Université Paris Descartes, Paris, France) for their services and help regarding the utilization of the UHPLC-MS/MS system for quantitative proteomics analysis. The authors would like to acknowledge the AIT imaging group (S. Mairinger, T. Filip, M. Sauberer, J. Stanek, A. Traxl and M. Löbsch) for support in performing the PET imaging part of this work.

Molecular Pharmacology Fast Forward. Published on February 18, 2016 as DOI: 10.1124/mol.115.102079
This article has not been copyedited and formatted. The final version may differ from this version.

Authorship Contributions

Participated in research design: DS, JK, JP, KD, LC, LL, LS, MM, NS, OL, SD, TW, XC, XD

Conducted experiments: AR, CA, CH, DGZ, EP, JP, JK, JY, MCM, MM, SC, TP, TW, XZ

Contributed new reagents or analytic tools: DGZ, MCM, XZ

Performed data analysis: CA, CH, DGZ, DS, EP, JK, JP, JY, KD, LC, LL, LS, MM, NS, MCM, OL, TP, TW, XC, XZ

Wrote or contributed to the writing of the manuscript: CA, DGZ, DS, EP, JK, KD, LC, KK, LS, MCM, MM, NS, OL, SD, TW, XC, XD

Molecular Pharmacology Fast Forward. Published on February 18, 2016 as DOI: 10.1124/mol.115.102079
This article has not been copyedited and formatted. The final version may differ from this version.

References

Allen JD, van Loevezijn A, Lakhai JM, van der Valk M, van Tellingen O, Reid G, Schellens JH, Koomen GJ and Schinkel AH (2002) Potent and specific inhibition of the breast cancer resistance protein multidrug transporter in vitro and in mouse intestine by a novel analogue of fumitremorgin C. *Mol Cancer Ther* **1**(6):417-425.

Bankstahl JP, Bankstahl M, Romermann K, Wanek T, Stanek J, Windhorst AD, Fedrowitz M, Erker T, Muller M, Loscher W, Langer O and Kuntner C (2013) Tariquidar and elacridar are dose-dependently transported by P-glycoprotein and Bcrp at the blood-brain barrier: a small-animal positron emission tomography and in vitro study. *Drug Metab Dispos* **41**(4):754-762.

Behringer R, Gertsenstein M, Nagy KV and Nagy A (2014) Manipulating the Mouse Embryo - A Laboratory Manual. *Cold Spring Harbor Laboratory Press* **Fourth Edition**:321-485.

Chambers KJ, Tonkin LA, Chang E, Shelton DN, Linskens MH and Funk WD (1998) Identification and cloning of a sequence homologue of dopamine beta-hydroxylase. *Gene* **218**(1-2):111-120.

Chan LM, Lowes S and Hirst BH (2004) The ABCs of drug transport in intestine and liver: efflux proteins limiting drug absorption and bioavailability. *Eur J Pharm Sci* **21**(1):25-51.

Chu X, Bleasby K and Evers R (2013) Species differences in drug transporters and implications for translating preclinical findings to humans. *Expert Opin Drug Metab Toxicol* **9**(3):237-252.

de Vries NA, Zhao J, Kroon E, Buckle T, Beijnen JH and van Tellingen O (2007) P-glycoprotein and breast cancer resistance protein: two dominant transporters working together in limiting the brain penetration of topotecan. *Clin Cancer Res* **13**(21):6440-6449.

Doyle L and Ross DD (2003) Multidrug resistance mediated by the breast cancer resistance protein BCRP (ABCG2). *Oncogene* **22**(47):7340-7358.

Enokizono J, Kusuhara H and Sugiyama Y (2007) Effect of Breast Cancer Resistance Protein (Bcrp/Abcg2) on the Disposition of Phytoestrogens. *Molecular Pharmacology* **72**(4):967-975.

European Medicine Agency (EMA) CfHMPC (2012) Guideline on the investigation of drug interactions. 21 June 2012.

Giacomini KM, Huang SM, Tweedie DJ, Benet LZ, Brouwer KL, Chu X, Dahlin A, Evers R, Fischer V, Hillgren KM, Hoffmaster KA, Ishikawa T, Keppler D, Kim RB, Lee CA, Niemi M, Polli JW, Sugiyama Y, Swaan PW, Ware JA, Wright SH, Yee SW, Zamek-Gliszczynski MJ and Zhang L (2010) Membrane transporters in drug development. *Nat Rev Drug Discov* **9**(3):215-236.

Gonzalez-Lobato L, Real R, Prieto JG, Alvarez AI and Merino G (2010) Differential inhibition of murine Bcrp1/Abcg2 and human BCRP/ABCG2 by the mycotoxin fumitremorgin C. *Eur J Pharmacol* **644**(1-3):41-48.

Hoshi Y, Uchida Y, Tachikawa M, Inoue T, Ohtsuki S and Terasaki T (2013) Quantitative atlas of blood-brain barrier transporters, receptors, and tight junction proteins in rats and common marmoset. *J Pharm Sci* **102**(9):3343-3355.

Hua WJ, Hua WX and Fang HJ (2012) The role of OATP1B1 and BCRP in pharmacokinetics and DDI of novel statins. *Cardiovasc Ther* **30**(5):e234-241.

Jani M, Makai I, Kis E, Szabo P, Nagy T, Krajcsi P and Lespine A (2011) Ivermectin interacts with human ABCG2. *J Pharm Sci* **100**(1):94-97.

Jonker JW, Buitelaar M, Wagenaar E, Van Der Valk MA, Scheffer GL, Scheper RJ, Plosch T,

Kuipers F, Elferink RP, Rosing H, Beijnen JH and Schinkel AH (2002) The breast cancer resistance protein protects against a major chlorophyll-derived dietary phototoxin and protoporphyria. *Proc Natl Acad Sci U S A* **99**(24):15649-15654.

Jonker JW, Smit JW, Brinkhuis RF, Maliepaard M, Beijnen JH, Schellens JH and Schinkel AH (2000) Role of breast cancer resistance protein in the bioavailability and fetal penetration of topotecan. *J Natl Cancer Inst* **92**(20):1651-1656.

Kamiie J, Ohtsuki S, Iwase R, Ohmine K, Katsukura Y, Yanai K, Sekine Y, Uchida Y, Ito S and Terasaki T (2008) Quantitative atlas of membrane transporter proteins: development and application of a highly sensitive simultaneous LC/MS/MS method combined with novel in-silico peptide selection criteria. *Pharm Res* **25**(6):1469-1483.

Kannan P, Telu S, Shukla S, Ambudkar SV, Pike VW, Halldin C, Gottesman MM, Innis RB and Hall MD (2011) The "specific" P-glycoprotein inhibitor Tariquidar is also a substrate and an inhibitor for breast cancer resistance protein (BCRP/ABCG2). *ACS Chem Neurosci* **2**(2):82-89.

Kitamura S, Maeda K, Wang Y and Sugiyama Y (2008) Involvement of multiple transporters in the hepatobiliary transport of rosuvastatin. *Drug Metab Dispos* **36**(10):2014-2023.

Kodaira H, Kusuhara H, Ushiki J, Fuse E and Sugiyama Y (2010) Kinetic analysis of the cooperation of P-glycoprotein (P-gp/Abcb1) and breast cancer resistance protein (Bcrp/Abcg2) in limiting the brain and testis penetration of erlotinib, flavopiridol, and mitoxantrone. *J Pharmacol Exp Ther* **333**(3):788-796.

Kusuhara H, Furuie H, Inano A, Sunagawa A, Yamada S, Wu C, Fukizawa S, Morimoto N, Ieiri I, Morishita M, Sumita K, Mayahara H, Fujita T, Maeda K and Sugiyama Y (2012) Pharmacokinetic interaction study of sulphasalazine in healthy subjects and the impact of curcumin as an in vivo inhibitor of BCRP. *Br J Pharmacol* **166**(6):1793-1803.

Lagas JS, van Waterschoot RA, Sparidans RW, Wagenaar E, Beijnen JH and Schinkel AH (2010) Breast cancer resistance protein and P-glycoprotein limit sorafenib brain accumulation. *Mol Cancer Ther* **9**(2):319-326.

Lai Y (2009) Identification of interspecies difference in hepatobiliary transporters to improve extrapolation of human biliary secretion. *Expert Opin Drug Metab Toxicol* **5**(10):1175-1187.

Lee SS, Jeong HE, Yi JM, Jung HJ, Jang JE, Kim EY, Lee SJ and Shin JG (2007) Identification and functional assessment of BCRP polymorphisms in a Korean population. *Drug Metab Dispos* **35**(4):623-632.

Leggas M, Adachi M, Scheffer GL, Sun D, Wielinga P, Du G, Mercer KE, Zhuang Y, Panetta JC, Johnston B, Scheper RJ, Stewart CF and Schuetz JD (2004) Mrp4 confers resistance to topotecan and protects the brain from chemotherapy. *Mol Cell Biol* **24**(17):7612-7621.

Leslie EM, Deeley RG and Cole SP (2005) Multidrug resistance proteins: role of P-glycoprotein, MRP1, MRP2, and BCRP (ABCG2) in tissue defense. *Toxicol Appl Pharmacol* **204**(3):216-237.

Li M, Yuan H, Li N, Song G, Zheng Y, Baratta M, Hua F, Thurston A, Wang J and Lai Y (2008) Identification of interspecies difference in efflux transporters of hepatocytes from dog, rat, monkey and human. *Eur J Pharm Sci* **35**(1-2):114-126.

Li N, Palandra J, Nemirovskiy OV and Lai Y (2009) LC-MS/MS mediated absolute quantification and comparison of bile salt export pump and breast cancer resistance protein in livers and hepatocytes across species. *Anal Chem* **81**(6):2251-2259.

Mazur CS, Marchitti SA, Dimova M, Kenneke JF, Lumen A and Fisher J (2012) Human and rat ABC transporter efflux of bisphenol a and bisphenol a glucuronide: interspecies comparison and implications for pharmacokinetic assessment. *Toxicol Sci* **128**(2):317-325.

Molecular Pharmacology Fast Forward. Published on February 18, 2016 as DOI: 10.1124/mol.115.102079
This article has not been copyedited and formatted. The final version may differ from this version.

Meyer zu Schwabedissen HE and Kroemer HK (2011) In vitro and in vivo evidence for the importance of breast cancer resistance protein transporters (BCRP/MXR/ABCP/ABCG2). *Handb Exp Pharmacol*(201):325-371.

Ni Z, Bikadi Z, Rosenberg MF and Mao Q (2010) Structure and function of the human breast cancer resistance protein (BCRP/ABCG2). *Curr Drug Metab* **11**(7):603-617.

Rostami-Hodjegan A (2012) Physiologically based pharmacokinetics joined with in vitro-in vivo extrapolation of ADME: a marriage under the arch of systems pharmacology. *Clin Pharmacol Ther* **92**(1):50-61.

Sadiq MW, Uchida Y, Hoshi Y, Tachikawa M, Terasaki T and Hammarlund-Udenaes M (2015) Validation of a P-Glycoprotein (P-gp) Humanized Mouse Model by Integrating Selective Absolute Quantification of Human MDR1, Mouse Mdr1a and Mdr1b Protein Expressions with In Vivo Functional Analysis for Blood-Brain Barrier Transport. *PLoS One* **10**(5):e0118638.

Silamut K, Molunto P, Ho M, Davis TM and White NJ (1991) Alpha 1-acid glycoprotein (orosomucoid) and plasma protein binding of quinine in falciparum malaria. *Br J Clin Pharmacol* **32**(3):311-315.

U.S. Department of Health and Human Services FaDA, Center for Drug Evaluation and Research (CDER). (2012.) Guidance for industry, drug interaction studies—study design, data analysis, implications for dosing, and labeling recommendations. . *http://wwwfdagov/downloads/Drugs/GuidanceComplianceRegulatoryInformation/Guidances/ucm292362pdf*.

Uchida Y, Ohtsuki S, Katsukura Y, Ikeda C, Suzuki T, Kamiie J and Terasaki T (2011) Quantitative targeted absolute proteomics of human blood-brain barrier transporters and receptors. *J Neurochem* **117**(2):333-345.

Urquhart BL, Ware JA, Tirona RG, Ho RH, Leake BF, Schwarz UI, Zaher H, Palandra J, Gregor JC, Dresser GK and Kim RB (2008) Breast cancer resistance protein (ABCG2) and drug disposition: intestinal expression, polymorphisms and sulfasalazine as an in vivo probe. *Pharmacogenet Genomics* **18**(5):439-448.

Wanek T, Kuntner C, Bankstahl JP, Mairinger S, Bankstahl M, Stanek J, Sauberer M, Filip T, Erker T, Muller M, Loscher W and Langer O (2012) A novel PET protocol for visualization of breast cancer resistance protein function at the blood-brain barrier. *J Cereb Blood Flow Metab* **32**(11):2002-2011.

Warren MS, Zerangue N, Woodford K, Roberts LM, Tate EH, Feng B, Li C, Feuerstein TJ, Gibbs J, Smith B, de Morais SM, Dower WJ and Koller KJ (2009) Comparative gene expression profiles of ABC transporters in brain microvessel endothelial cells and brain in five species including human. *Pharmacol Res* **59**(6):404-413.

Yamasaki Y, Ieiri I, Kusuhara H, Sasaki T, Kimura M, Tabuchi H, Ando Y, Irie S, Ware J, Nakai Y, Higuchi S and Sugiyama Y (2008) Pharmacogenetic characterization of sulfasalazine disposition based on NAT2 and ABCG2 (BCRP) gene polymorphisms in humans. *Clin Pharmacol Ther* **84**(1):95-103.

Zaher H, Khan AA, Palandra J, Brayman TG, Yu L and Ware JA (2006) Breast cancer resistance protein (Bcrp/abcg2) is a major determinant of sulfasalazine absorption and elimination in the mouse. *Mol Pharm* **3**(1):55-61.

Zamek-Gliszczynski MJ, Bedwell DW, Bao JQ and Higgins JW (2012a) Characterization of SAGE Mdr1a (P-gp), Bcrp, and Mrp2 knockout rats using loperamide, paclitaxel, sulfasalazine, and carboxydichlorofluorescein pharmacokinetics. *Drug Metab Dispos* **40**(9):1825-1833.

Zamek-Gliszczynski MJ, Hoffmaster KA, Tweedie DJ, Giacomini KM and Hillgren KM (2012b) Highlights from the International Transporter Consortium second workshop. *Clin Pharmacol Ther* **92**(5):553-556.

Zhang W, Yu BN, He YJ, Fan L, Li Q, Liu ZQ, Wang A, Liu YL, Tan ZR, Fen J, Huang YF

Molecular Pharmacology Fast Forward. Published on February 18, 2016 as DOI: 10.1124/mol.115.102079
This article has not been copyedited and formatted. The final version may differ from this version.

and Zhou HH (2006) Role of BCRP 421C>A polymorphism on rosuvastatin pharmacokinetics in healthy Chinese males. *Clin Chim Acta* **373**(1-2):99-103.

Zhang Y, Buchholz F, Muyrers JP and Stewart AF (1998) A new logic for DNA engineering using recombination in Escherichia coli. *Nat Genet* **20**(2):123-128.

Molecular Pharmacology Fast Forward. Published on February 18, 2016 as DOI: 10.1124/mol.115.102079
This article has not been copyedited and formatted. The final version may differ from this version.

Footnotes

SD and LS contributed equally to this paper.

The PET imaging part of this work was supported by the Austrian Science fund (FWF) [Grants P24894-B24 and F 3513-B20].

Reprint requests:

Laurent Salphati, Pharm.D., PhD, Department of Drug Metabolism and Pharmacokinetics, Genentech, Inc., 1 DNA Way, South San Francisco, CA 94080, USA.

Tel.: 650-467-1796; Fax: 650-467-3487; Email: salphati.laurent@gene.com

Molecular Pharmacology Fast Forward. Published on February 18, 2016 as DOI: 10.1124/mol.115.102079
This article has not been copyedited and formatted. The final version may differ from this version.

Figure Legends

Fig. 1 Strategy to generate hBCRP and Bcrp$^{-/-}$ mice. (A) Genomic organisation of the mouse *Bcrp* gene locus. The start ATG and stop codon are shown. (B) Vector used for targeting of *Bcrp* by homologous recombination in mouse ES cells. (C) Genomic organisation of *Bcrp* in targeted ES cells after homologous recombination. (D) *Bcrp* gene locus in the hBCRP model after Flp-mediated deletion of the neomycin (Neo) and puromycin (Puro) expression cassettes. (E) *Bcrp* gene locus in the Bcrp$^{-/-}$ model after Cre-mediated deletion of human *BCRP* exons 3-15. For the sake of clarity sequences of the targeting vectors are not drawn to scale.

Fig. 2 Relative murine *Bcrp* and human *BCRP* mRNA expression levels in WT and hBCRP mice. RNA was isolated from WT and hBCRP male (black bars) and female (grey bars) mice (n=3 for each line and sex). Murine *Bcrp* and human *BCRP* mRNA expression was analyzed by quantitative PCR (TaqMan) in liver (A), brain (B), kidney (C), duodenum (D), colon (E) and testis (F) and normalized to murine β-actin. Relative mRNA levels were assessed by a comparative ($2^{-\Delta\Delta CT}$) approach as described in the Supplemental Materials and Methods section. Values represent the mean expression level ± SD with expression levels of the murine *Bcrp* mRNA in WT males arbitrarily set as 1.

Fig. 3 Sulfasalazine blood concentration-time profiles in WT, hBCRP and Bcrp$^{-/-}$ mice. Pharmacokinetic profile after 5 mg/kg iv (A) or 20 mg po (B, C) administration of sulfasalazine to male WT (black diamond), hBCRP mice (dark grey triangle) and Bcrp1$^{-/-}$ (light grey circle). Sulfasalazine was administered in the absence (A, B) or presence (C) of the BCRP inhibitor Ko143 (20 mg/kg). Sulafasalazine concentrations-time profiles in the presence of Ko143 are represented as dotted lines (C). Values shown are mean ± SD of n=4

Molecular Pharmacology Fast Forward. Published on February 18, 2016 as DOI: 10.1124/mol.115.102079
This article has not been copyedited and formatted. The final version may differ from this version.

mice per strain.

Fig. 4 Daidzein plasma concentration-time profiles and brain and plasma concentrations in WT, hBCRP and Bcrp$^{-/-}$ mice. 5 mg/kg daidzein was administered IV to male mice. (A) Pharmacokinetic profiles in WT (black triangles), hBCRP (dark grey diamonds) and Bcrp$^{-/-}$ mice (light grey squares). (B) $AUC_{0\text{-}1hr}$ values in WT (black bar), hBCRP (dark grey bar) and Bcrp$^{-/-}$ mice (light grey bar). (C-E) Plasma (black bars) and brain (grey bars) concentrations at (C) 30 minutes, (D) 1 hour and (E) 2 hours after daidzein administration. Values shown in (A) and (C-E) are mean ± SD with n=3 mice per strain and time point for (A) and n=2 mice per strain and time point for (C-E). *, $P < 0.05$, statistically significant compared to indicated control mice. $AUC_{0\text{-}1hr}$ (B) are mean (±SD; n=3 mice per strain); *, $P<0.05$, statistically significant compared to indicated control mice.

Fig. 5 Genistein blood concentration-time profiles and brain and blood concentrations in WT, hBCRP and Bcrp$^{-/-}$ mice. Pharmacokinetic profiles in WT (black circles), hBCRP (black triangles) and Bcrp$^{-/-}$ male mice (white circles) following (A) 20 mg/kg intravenous, (B) 20 mg/kg oral or (C) 50 mg/kg oral administration of genistein, respectively. (D and E) Genistein blood (black bars) and brain (grey bars) concentrations (D) 15 minutes and (E) 90 minutes after 20 mg/kg intravenous administration. (F) Genistein brain-to-blood concentration ratio in WT (black bars), hBCRP (grey bars) and Bcrp$^{-/-}$ (white bars) mice 15 and 90 minutes after 20 mg/kg intravenous administration. Values shown are mean ± SD with n=8 (A-C) or n=4 (D-F) mice per strain and time point. *, $P < 0.05$, statistically significant compared to Bcrp$^{-/-}$ mice.

Fig. 6 Rosuvastatin blood concentration-time profiles in WT, hBCRP and Bcrp$^{-/-}$ mice. Pharmacokinetic profiles in WT (black diamonds), hBCRP (black triangles) and Bcrp$^{-/-}$ male mice (white squares) following (A) 6.1 mg/kg intravenous and (B) 13.7 mg/kg oral

Molecular Pharmacology Fast Forward. Published on February 18, 2016 as DOI: 10.1124/mol.115.102079
This article has not been copyedited and formatted. The final version may differ from this version.

administration of rosuvastatin, respectively. Values shown are mean ± SD with n=4 mice per strain and time point.

Fig. 7 Topotecan blood concentration-time profiles and brain and blood concentrations in WT, hBCRP and Bcrp$^{-/-}$ mice. Pharmacokinetic profiles in WT (black diamonds), hBCRP (black triangles) and Bcrp$^{-/-}$ male mice (white squares) following (A) 1 mg/kg intravenous or (B) 1 mg/kg oral administration of topotecan, respectively. (C and D) Topotecan brain concentrations (C) 15 and (D) 60 minutes after 1 mg/kg oral administration. (E) Topotecan brain-to-blood concentration ratio in WT (black bars), hBCRP (grey bars) and Bcrp$^{-/-}$ (white bars) mice 15 and 60 minutes after 1 mg/kg oral administration. Values shown are mean ± SD with n=8 for WT and hBCRP and n=7 for Bcrp$^{-/-}$ (A), n=8 for Bcrp$^{-/-}$ and hBCRP and n=7 for WT (B), n=4 for each mouse line (C), n=4 for Bcrp$^{-/-}$ and hBCRP and n=3 for WT (D), and n=4 for WT and Bcrp$^{-/-}$ at 15 minutes and Bcrp$^{-/-}$ at 60 minutes and n=3 for WT at 60 minutes and hBCRP at 15 and 60 minutes. *, $P < 0.05$, statistically significant compared to Bcrp$^{-/-}$ mice.

Fig. 8 Sagittal PET summation images (0-60 min) and mean (± SD) time-activity curves of [^{11}C]tariquidar in hBCRP (A, B) and C57BL/6N WT mice (C, D) pretreated iv with tariquidar (TQD) and Ko143 vehicle (veh/veh) or tariquidar (12 mg/kg) and Ko143 vehicle (TQD/veh) or tariquidar (12 mg/kg) and Ko143 (10 mg/kg) (TQD/Ko143) (n = 4-6 per group). Tariquidar was administered at 2 hours and Ko143 at 1 hour before start of the PET scan. Whole brain region which was used for image quantification is highlighted (red broken line). All images are set to the same intensity scale (0-4 standardized uptake value, SUV). In (E) mean (+SD) brain-to-blood radioactivity concentration ratios at the end of the PET scan ($K_{b,brain}$) are shown (***, $P<0.001$, 1-way ANOVA followed by Bonferroni´s multiple comparison test).

Molecular Pharmacology Fast Forward. Published on February 18, 2016 as DOI: 10.1124/mol.115.102079
This article has not been copyedited and formatted. The final version may differ from this version.

Tables

TABLE 1

Expression of BCRP/Bcrp and Na^+/K^+ ATPase proteins in mouse Kidney, Liver and Cortical vessels obtained by AQUA quantification by UHPLC-MS/MS.

		Expression per sample group in fmol/µg of total protein (%CV)	
Tissue	**Mouse line**	**Bcrp/BCRP**	**Na+/K+ ATPase**
Liver (PMF)	WT	1.55 (7.6%)	15.6 (8.9%)
	hBCRP	0.726 (12.6%)	17.1 (8.63%)
Kidney (PMF)	WT	37.7 (9.07%)	317 (24.9%)
	hBCRP	9.34 (14.5%)	231 (13.6%)
Cortical vessels (WL)	WT	0.225 (44.0%)	26.4 (31.9%)
	hBCRP	0.393 (17.4%)	29.1 (32.9%)

PMF = plasma membrane fraction; WL = whole lysate

Data are presented as the mean of the calculated value for the digestion replicates of each sample. Therefore, the %CV represents the variability between samples and digestion replicates. The analytical %CV corresponding to the digestion reproducibility was inferior to 20% in all the samples. For liver and kidney samples from 3 different mice per line were used and each sample was digested in triplicate. For cortical vessels samples from 2 WT and 3 hBCRP mice were used and each sample was digested from one to three replicates, depending on the protein amount obtained after vessel isolation.

Figure 1

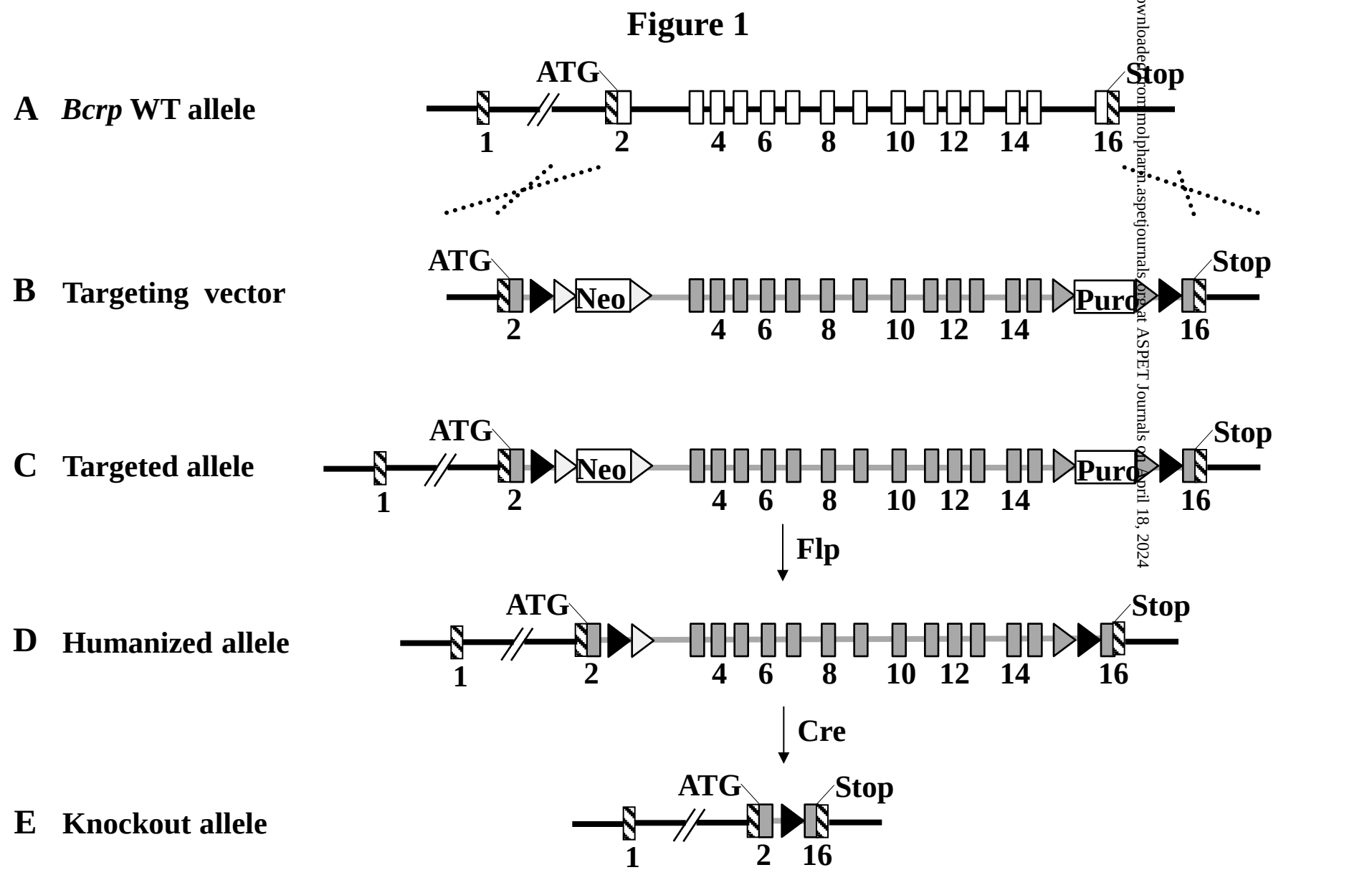

Figure 2

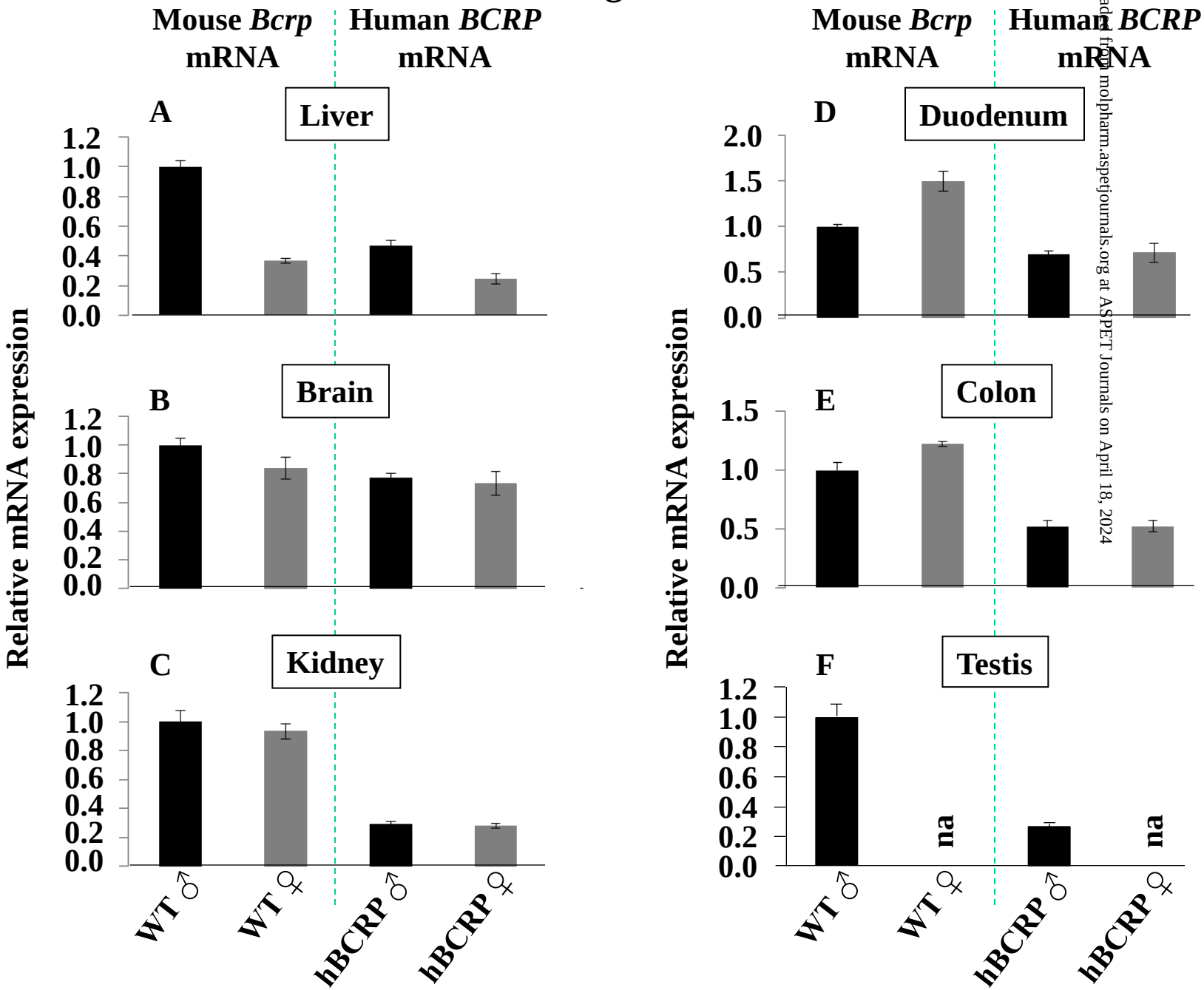

Figure 3

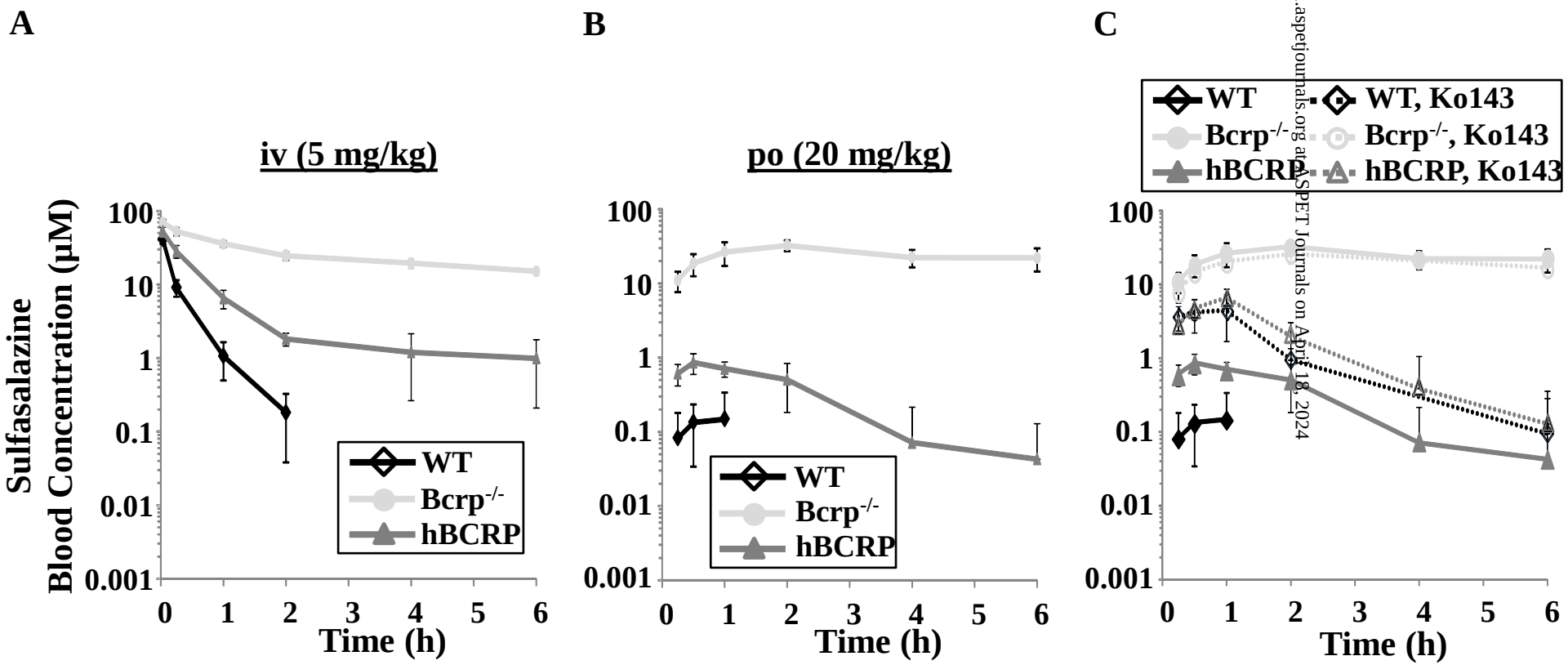

Figure 4

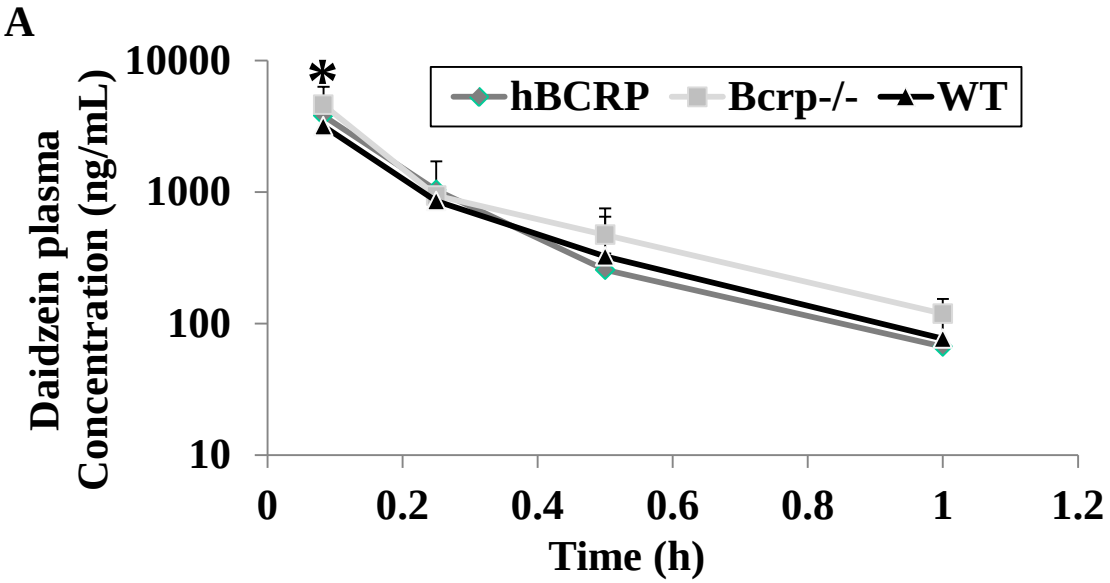

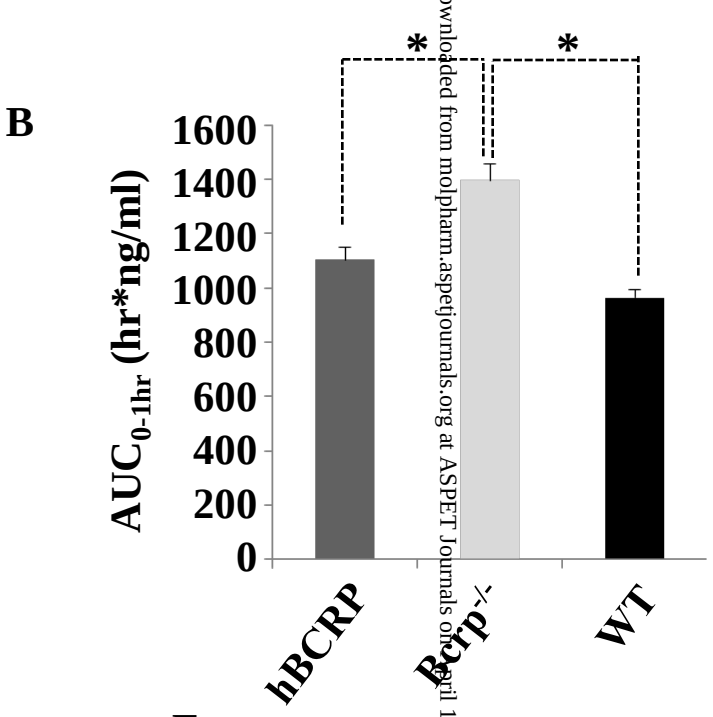

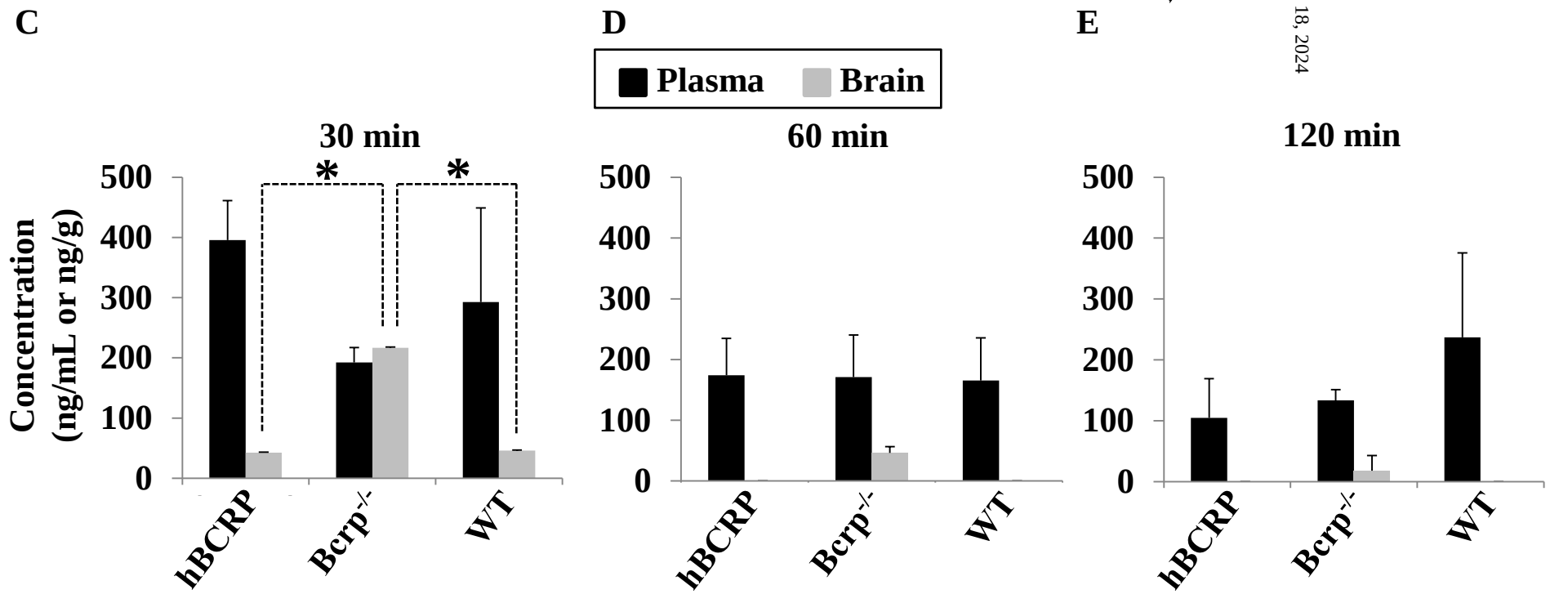

Figure 5

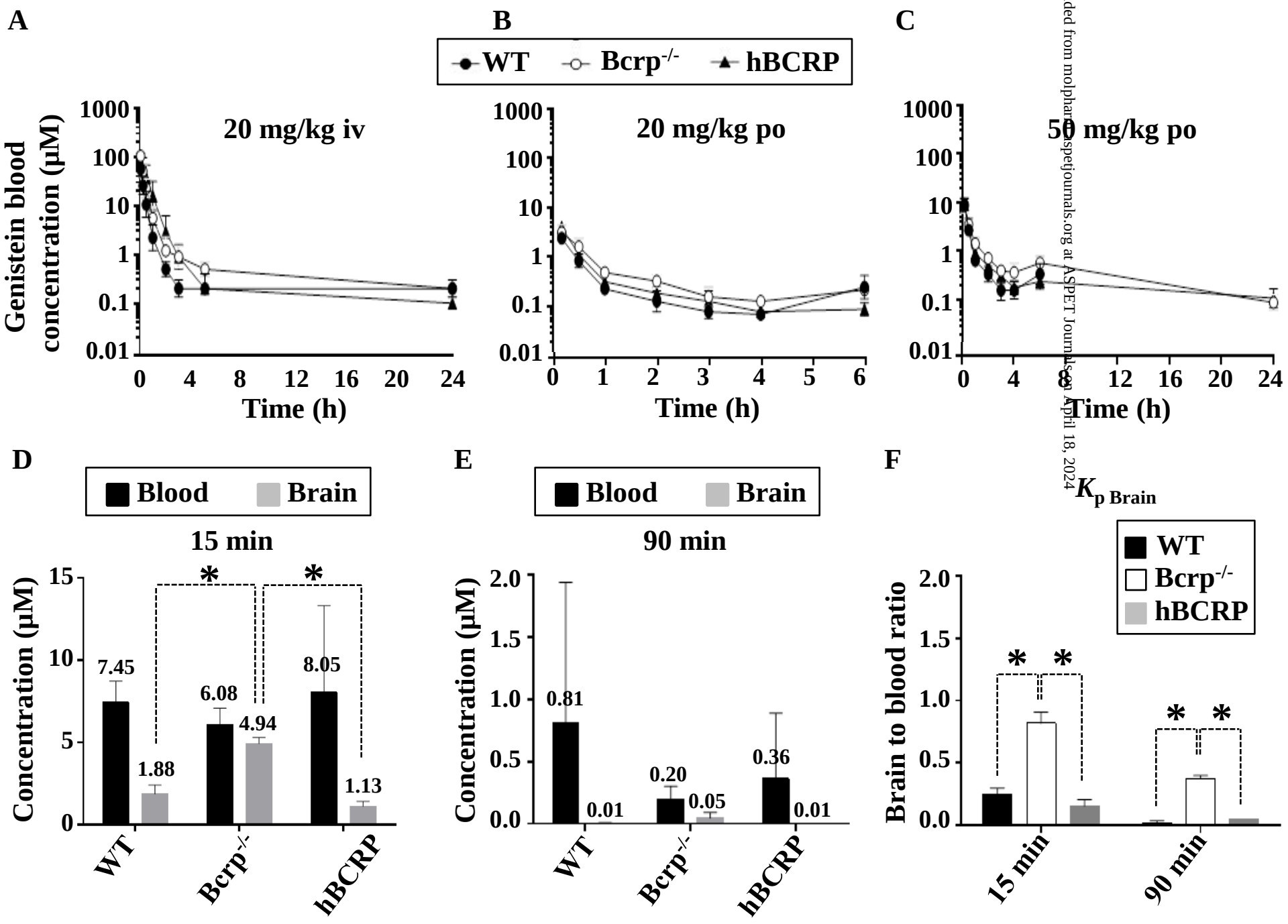

Figure 6

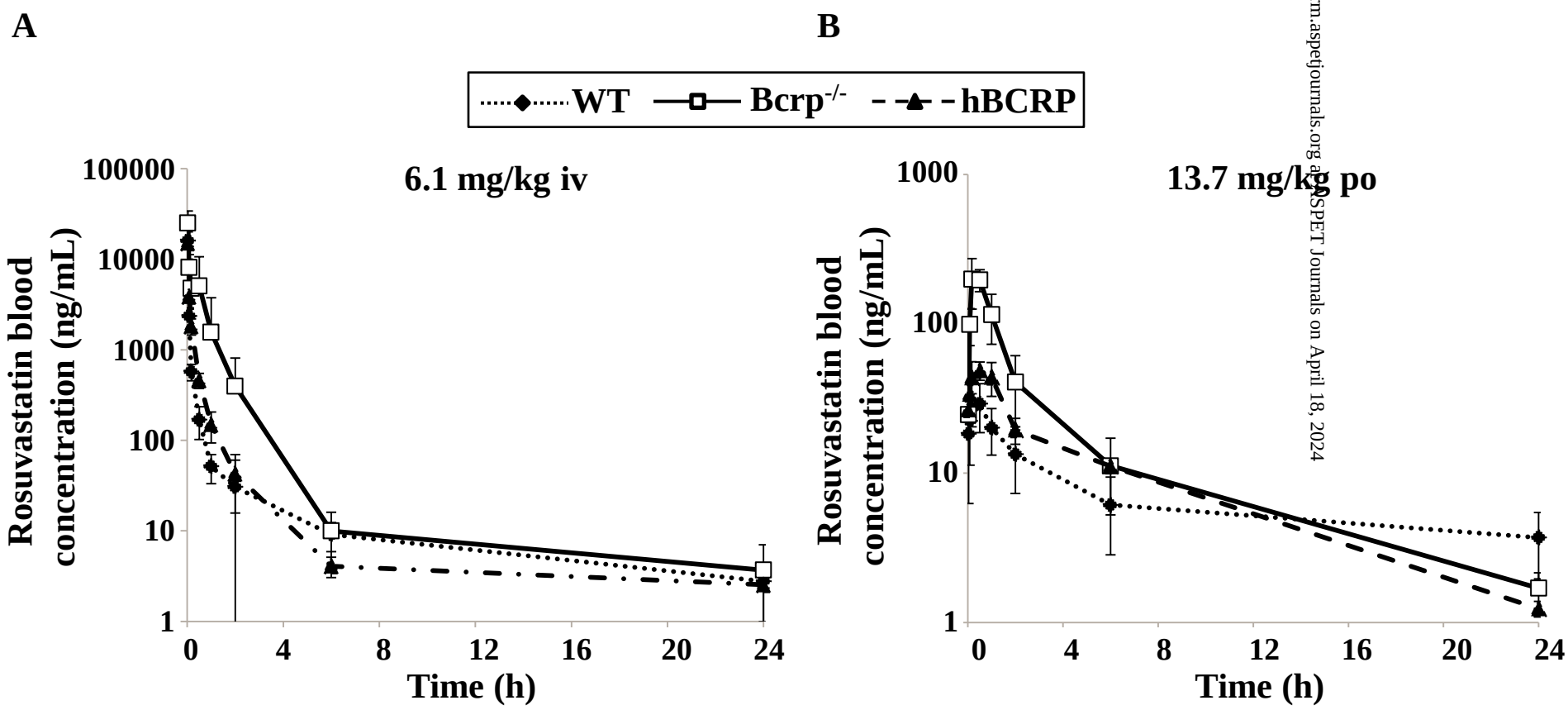

Figure 7